# Nanoscale

Accepted Manuscript


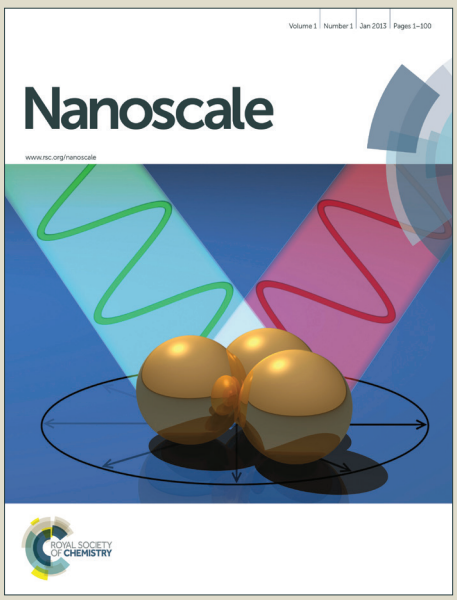





ROYAL SOCIETY OF CHEMISTRY

www.rsc.org/nanoscale

Cite this: DOI: 10.1039/c0xx00000x

www.rsc.org/xxxxxx

FEATURE ARTICLE

# Enzymatically induced motion at nano- and microscale

**Szilveszter Gáspár*[a]**

***Received (in XXX, XXX) Xth XXXXXXXXX 20XX, Accepted Xth XXXXXXXXX 20XX***
**DOI: 10.1039/b000000x**

In contrast to adenosine triphosphate (ATP)-dependent motor enzymes, other enzymes are little-known as "motors" or "pumps", that is, for their ability to induce motion. The enhanced diffusive movement of enzyme molecules, the self-propulsion of enzyme-based nanomotors, and liquid pumping with enzymatic micropumps were indeed only recently reported. Enzymatically induced motion can be achieved in mild conditions and without the use of external fields. It is thus better suited for use in living systems (from single-cell to whole-body) than most other ways to achieve motion at small scale. Enzymatically induced motion is thus not only new but also important. Therefore, the present work reviews the most significant discoveries in enzymatically induced motion. As we will learn, freely diffusing enzymes enhance their diffusive movement by nonreciprocal conformational changes which parallel their catalytic cycles. Meanwhile, enzyme-modified nano- and microobjects turn chemical energy into kinetic energy through mechanisms such as bubble recoil propulsion, self-electrophoresis, and self-diffusiophoresis. Enzymatically induced motion of small objects ranges from enhanced diffusive movement to directed motion at speeds as high as 1 cm $s^{-1}$. In spite of the progress made in understanding how the energy of enzyme reactions is turned into motion, most enzymatically powered devices remain inefficient and need improvements before we will witness their application in real world environments.

## 1. Introduction

The development of "motors" small enough to fit nanometer- and micrometer-sized "vehicles" and of autonomous "pumps" small enough to fit into the tiniest fluid channels is expected to lead to devices with multiple functions which will radically change the way we diagnose, monitor, and cure diseases. Therefore, a significant research effort is currently directed toward developing such motors and pumps. This effort has resulted in a good number of fully synthetic nanomotors which have been nicely reviewed elsewhere [1–4]. Most synthetic nanomotors induce motion by creating a concentration gradient along their body. Some nanomotors create their local concentration gradient indirectly, for example under the effect of an electric field [5] or by creating first a local temperature gradient [6]. Catalytic nanomotors carry chemically active zones which convert species from their surroundings. They are thus able to produce concentration gradients without any external field. This is very convenient because applying an external field requires additional equipment and is not always possible. Thus, not surprisingly, catalytic nanomotors are among the most popular nanomotors. The recently reported catalytic nanomotors self-propel if surrounded by fuel such as hydrazine [7], hydrogen peroxide [8], or bromine (iodine) [9].

In spite of this progress, we are far from using miniaturized motors or pumps to carry out complex studies and interventions in living systems, be it a single-cell or a whole-body. The main reasons of this fact are the size, the inability to deal with real-world samples [10,11], and, last but not least, the poor biocompatibility of the great majority of miniaturized motors and pumps developed up to now. This poor biocompatibility made researchers turn their attention to enzymes. Although there is a great diversity of enzymes characterized by amazing turnover numbers and excellent selectivity in physiological conditions, only few motors and pumps based on enzyme catalysis have been developed. These represent a significant step toward devices characterized by biocompatibility and will be reviewed in the present work. Adenosine triphosphate (ATP)-dependent motor proteins (such as kinesin, myosin, and dynein) are intensively studied and used to develop hybrid (bio – non-bio) nanodevices. Reviewing those devices is not within the scope of this work that will focus on structures using enzymes with physiological roles other than inducing motion. The hybrid devices using ATP-dependent biological motor proteins are reviewed elsewhere [12].

## 2. Motion induced with immobilized enzymes

Listeria monocytogenes moves inside host cells through the polymerization of actin with actin assembly-inducing protein (ActA), a protein that is distributed on the bacterial surface in a polar fashion (i.e. asymmetrically). Aiming for a better understanding of the way this pathogen moves, researchers have created some of the first protein-propelled nanomachines by modifying the surface of polystyrene beads with purified ActA [13].

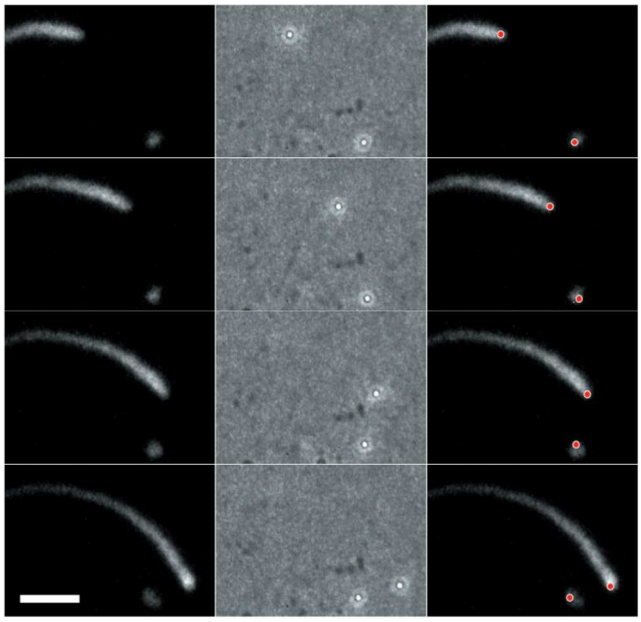

**Fig. 1** Actin-based movement of a 0.5 µm diameter polystyrene bead uniformly coated with ActA protein and suspended in cytoplasmic extract supplemented with fluorescent actin. The frames are separated by 30 s from each other. The fluorescence images in the left column show the distribution of fluorescent-actin in the comet tail. The phase-contrast images in the centre column show the positions of two polystyrene beads (one of them stationary). The right column presents bead positions (red dots) superimposed on fluorescence images. The scale bar corresponds to 5 µm. (Reprinted by permission from L. A. Cameron, M. J. Footer, A. van Oudenaarden, and J. A. Theriot, Proc. Natl. Acad. Sci., 1999, 96, 4908–4913., Copyright 1999 National Academy of Sciences, U.S.A)

These ActA-modified polystyrene beads moved in actin-rich cytoplasmic extracts with an average speed of 0.119 µm $s^{-1}$ when their diameter was 0.5 µm (Figure 1). However, when polystyrene beads as large as 2 µm were taken into work, protein ActA had to be immobilized onto the beads in a polar fashion in order to induce their motion. It is thus clear, that the ActA-mediated polymerization of actin must produce an inhomogeneous distribution of species in the vicinity of the bead in order to allow the diffusiophoretic mechanism to operate, and thus the bead to propel itself. When using a 2 µm large bead, this inhomogeneous distribution of species was achieved only when ActA protein was asymmetrically immobilized onto the bead. That asymmetry is required for directed motion was subsequently several times demonstrated with different structures. Because the movement of particles driven by an applied concentration gradient is called diffusiophoresis, the movement of particles by self-generated concentration gradients was named self-diffusiophoresis. The speed (U) of a charged particle subjected to an electrolyte concentration gradient (applied externally or self-generated) is given by the following equation (see [14] and references therein):

$$U = \frac{\varepsilon\zeta}{4\pi\eta}\frac{kT}{Ze}\frac{\nabla n^{\infty}}{n^{\infty}(0)}(\alpha + \overline{\zeta}^{-1} ln\, cosh\overline{\zeta})$$

$$\alpha = \frac{D_2 - D_1}{D_2 + D_1}$$

$$\overline{\zeta} = \frac{Ze\zeta}{4kT}$$

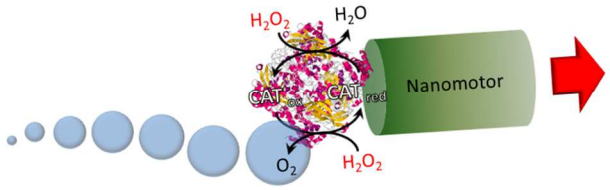


**Fig. 2** Self-propulsion of catalase (CAT)-modified nano- and microobjects due to the recoil from the oxygen bubbles resulting from the decomposition of hydrogen peroxide. The direction of motion is indicated by the large red arrow. *Important to note*: Catalase is both oxidized and reduced by hydrogen peroxide and thus it requires no co-substrate. Hydrogen peroxide is needed in high concentrations (≥ 1.5%) for catalase to form oxygen bubbles. Hydrogen peroxide can result from an oxidase also immobilized onto the surface of the nanomotor (as shown in [21]).

where $\varepsilon/4\pi$ is the solution permittivity, $\zeta$ is the zeta potential of the particle, $\eta$ is the solution viscosity, $k$ is the Boltzmann constant, $T$ is the absolute temperature, $Z$ is the absolute value of the valences of the ions, $e$ is the charge of a proton, $\nabla n^{\infty}$ is the concentration gradient, $n^{\infty}(0)$ is the electrolyte concentration at the particle centre in the absence of the particle, and $D_1$ and $D_2$ are the diffusion coefficients of the anion and the cation, respectively. While this equation does not apply to all structures presenting diffusiophoresis it gives a good overview of the parameters which impact the phenomenon.

Self-propulsion by decomposition of hydrogen peroxide was first demonstrated in 2002 by the group of G. M. Whitesides from Harvard University [15]. Their 9 mm diameter poly(dimethylsiloxane) plate was carrying a 2 mm x 2 mm piece of platinized porous glass and was moving at the surface of an aqueous solution of 3% hydrogen peroxide. Pt catalyzed the decomposition of hydrogen peroxide ($2\ H_2O_2 \rightarrow O_2 + 2\ H_2O$), and the whole structure moved due to the recoil from the $O_2$ bubbles departing from the surface of the platinized porous glass. Catalase is the biochemical equivalent of Pt when it comes to decomposition of hydrogen peroxide. This enzyme consists of four subunits (60 kDa each), decomposes hydrogen peroxide at rates approaching the diffusion-controlled limit, and thus is one of the most efficient enzymes known [16]. Therefore is not surprising that, shortly after the publication of Whitesides's paper, catalase-based biochemical self-propulsion was also reported. First a synthetic catalase was used to modify 80 µm $SiO_2$ particles and thus achieve their self-propulsion at speeds as high as 35 µm $s^{-1}$ [17]. Natural enzymes lose their activity quite fast once purified. Therefore, synthetic enzymes represent a promising way to gain long-term stability of enzyme-based motors and pumps (given the synthetic enzyme reproduces the selectivity and activity of its natural counterpart). The synthetic catalase-modified $SiO_2$ particles were shown to self-propel in very high concentrations of hydrogen peroxide (5%) and in organic solvent (acetonitrile). This medium is clearly not something a nanomotor can meet in biological systems.

Non-synthetic catalase–based "microengines", showing directed motion in hydrogen peroxide solution, were also reported few years later [18]. The microengines were made by rolling up titanium / gold films to obtain 25 µm long microtubes, and by covalently attaching catalase to the golden inner part of

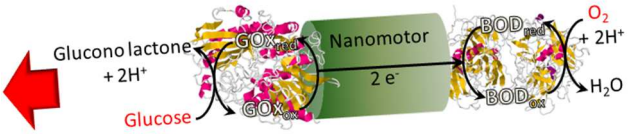


**Fig. 3** Self-propulsion of a glucose oxidase (GOx)- and bilirubin oxidase (BOD)-based nanomotor due to bioelectrochemically induced self-electrophoresis resulting from the simultaneous conversion of glucose and oxygen. The direction of motion is indicated by the large red arrow. *Important to note*: Neither glucose oxidase nor bilirubin oxidase is able of direct electron transfer to solid electrodes. Therefore, in the actual device redox polymers were used to mediate electron transfer to / from these enzymes [23]. In a more recent structure, glucose oxidase was replaced with cytochrome c and bilirubin oxidase with horseradish peroxidase. The resulting structure has shown bioelectrochemically induced self-electrophoresis in presence of superoxide, and hydrogen peroxide (instead of glucose and oxygen) [24].

these microtubes. Due to their complex design, the catalase-based microengines were more efficient than the nanomotors made with synthetic catalase, and moved with an average speed of ~ 200 µm $s^{-1}$ if dispersed into a solution containing 1.5% hydrogen peroxide. These microengines represent an important progress compared to the nanomotors with synthetic catalase. However, the hydrogen peroxide concentration required for their directed motion is still too high to be compatible with living cells. While catalase-based nanomotors are not yet compatible with living cells, they have found applications in the capture and transport of DNA-modified objects [19], and determination of water quality [20]. The last application is based on the inhibition of catalase by toxic compounds, inhibition that negatively affects the propulsion speed of catalase-based nanomotors.

A little bit better biocompatibility is characterizing the glucose oxidase- and catalase-modified carbon nanotube aggregates and bundles self-propelling in glucose [21]. Glucose oxidase is a dimeric enzyme that converts glucose and oxygen, into glucono lactone and hydrogen peroxide, respectively [22]. Therefore, the self-propulsion of these 200-800 nm long aggregates and bundles in glucose solutions is due to the hydrogen peroxide produced by glucose oxidase and then consumed by catalase with formation of oxygen bubbles. The achieved propulsion rates are again great (0.2 - 0.8 cm $s^{-1}$) but the concentration of the fuel needed for propulsion is one which is still difficult to find in biological systems (100 mM glucose). Using poorly defined nanotube aggregates and bundles is also not very advantageous (because they are difficult the reproduce). The reaction cascade self-propelling catalase-modified nano- and microobjects is schematically depicted in Figure 2.

There are very few nano- or microobjects with motion induced through the use of other enzymes than catalase. Probably the most notorious of these objects are the carbon fibers, with one end modified with glucose oxidase and the other end modified with bilirubin oxidase, which show self-propulsion at the surface of an aqueous solution of glucose (2 - 32 mM) [23]. The speed of the self-propulsion of these fibers is impressive (1 cm $s^{-1}$) but the fibers are large (0.5 – 1 cm), manually modified with enzymes, and their movement is restricted to 3 minutes and to the surface of the glucose solution. All these features make the structure a poor candidate for biological applications. The structure is still of great importance because of its mechanism of self-propulsion that

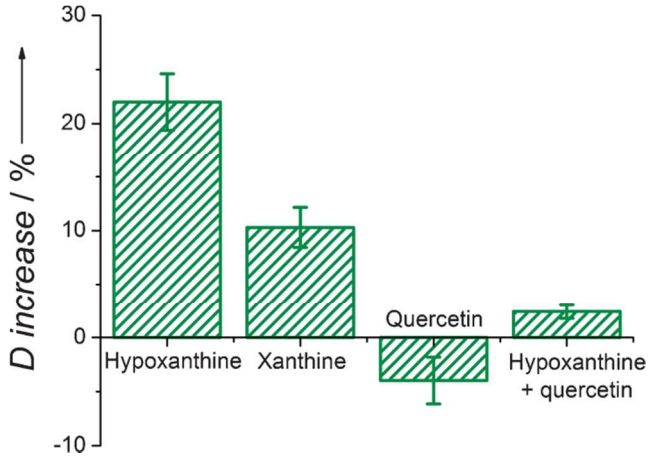


**Fig. 4** Comparison of the relative diffusion coefficients of horseradish peroxidase- and cytochrome c-modified nanorods suspended in solutions with xanthine oxidase (300 mU $mL^{-1}$) and hypoxanthine (200 µM), xanthine (200 µM), quercetin (200 µM), or quercetin and hypoxanthine (200 µM each). *Important to note*: Xanthine oxidase converts hypoxanthine with the production of both hydrogen peroxide and superoxide. When the production of reactive oxygen species was decreased by using xanthine instead of hypoxanthine or by using an inhibitor of xanthine oxidase, the diffusion coefficient of the nanorods increased into a smaller extent or did not increase at all. (Reprinted by permission from I.-A. Pavel, A.-I. Bunea, S. David, and S. Gáspár, ChemCatChem, 2014, 6, 866–872. Copyright 2014 John Wiley & Sons, Inc.)

is completely different from the bubble recoil mechanism powering catalase-based structures (and from the self-diffusiophoresis powering the early ActA-based motors described above). Glucose oxidase- and bilirubin oxidase-modified carbon fibers gain kinetic energy by a mechanism most often called self-electrophoresis. Movement of charged particles in a solution, driven by an applied electric field is called electrophoresis. Self-electrophoresis is thus the movement of charged particles driven by a self-generated electric field. The speed (U) of a charged particle presenting electrophoresis (or self-electrophoresis) is given by the following equation (see [14] and references therein):

$$U = \frac{\varepsilon\zeta}{4\pi\eta}E$$

where $\boldsymbol{\varepsilon}/4\pi$ is the solution permittivity, $\zeta$ is the zeta potential of the particle, $\eta$ is the solution viscosity, and E is the applied (or self-generated) electric field. While this equation does not apply to all structures presenting electrophoresis it gives a good overview of the parameters which impact the phenomenon. Self-electrophoresis of the above enzyme-modified fiber involves i.) an oxidation reaction occurring at one end of the fiber (i.e. oxidation of glucose by glucose oxidase), ii.) a reduction reaction occurring at the other end of the fiber (i.e. reduction of oxygen by bilirubin oxidase), and iii.) a current flow through the fiber (from glucose oxidase to bilirubin oxidase). As a result of these three processes, protons travel in the electrical double layer of the fiber, from the glucose oxidase-modified end of the fiber to the bilirubin oxidase modified end, dragging water molecules with them. Motion of the liquid adjacent to the nanomotor propels the nanomotor in the opposite direction. The reaction cascade self-propelling this glucose oxidase- and bilirubin oxidase-based nanomotor through self-electrophoresis is schematically depicted in Figure 3.

Cite this: DOI: 10.1039/c0xx00000x

www.rsc.org/xxxxxx

# FEATURE ARTICLE

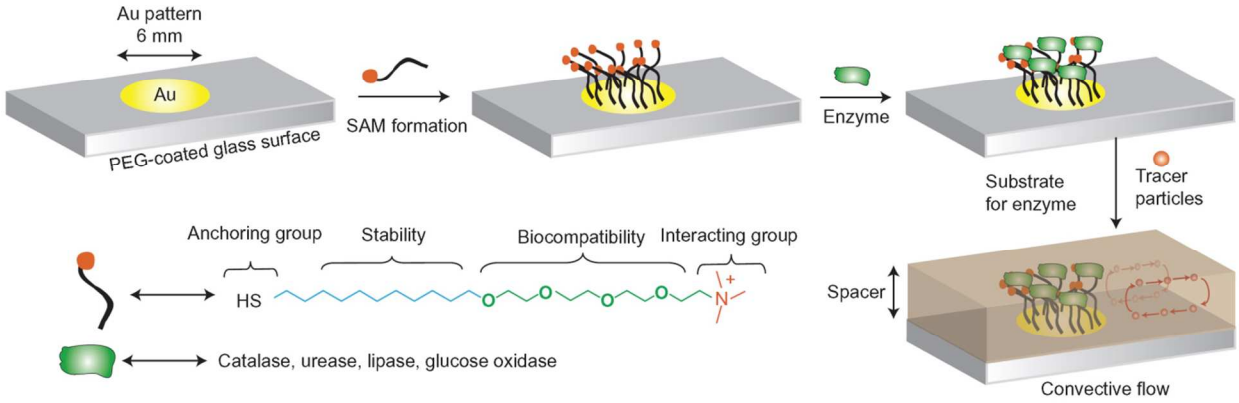


**Fig. 5** Fluid pumping using a small immobilized enzyme spot developed inside the fluidic channel. *Important to note*: Such autonomous micropumps will turn ON only in the presence of the substrate of the immobilized enzyme. Moreover, their pumping speed will be advantageously dependent on the concentrations of the enzyme substrate. (Reprinted by permission from S. Sengupta, D. Patra, I. Ortiz-Rivera, A. Agrawal, S. Shklyaev, K. K. Dey, U. Córdova-Figueroa, T. E. Mallouk, and A. Sen, Nat. Chem., 2014, 6, 415–422. Copyright 2014 Macmillan Publishers Ltd).

Nanorods with a polypyrrole segment and a gold segment made by template assisted electrodeposition were recently modified with either one or two of the following hemeproteins: horseradish peroxide, catalase, and cytochrome c [25]. Modification with a given hemeprotein was always restricted to one of the two segments. The used hemeproteins are all able to convert hydrogen peroxide by either peroxidase-like or catalase-like activity, depending on the experimental conditions. Because of this ability of the hemeproteins, the hemeprotein-modified nanorods were characterized by diffusion coefficients which increased with the hydrogen peroxide concentration (up to 10 mM hydrogen peroxide at least). For example, the nanorod with its polypyrrole segment modified with horseradish peroxidase has enhanced its diffusion coefficient with 16% in 10 mM hydrogen peroxide as compared to its coefficient in water. Unmodified nanorods, and nanorods symmetrically modified with only one hemeprotein, do not show such behavior. Interestingly, the results also show that the enhanced diffusive movement of the hemeprotein-modified nanorods is most probably due to self-diffusiophoresis in the case of the nanorod carrying horseradish peroxidase on its polypyrrole segment, and due to self-electrophoresis in the case of the other investigated nanorods. However, the observed self-electrophoresis was lacking the support of a significant current through the hemeprotein-modified nanorod. This situation was partially rectified when the horseradish peroxidase- and cytochrome c-modified nanorods were suspended in mixtures of superoxide and hydrogen peroxide [24]. Superoxide and hydrogen peroxide are two biologically important reactive oxygen species which were produced with xanthine oxidase and hypoxanthine in order to test the nanorods. In the presence of superoxide and hydrogen peroxide the horseradish peroxidase- and cytochrome c-modified nanorods combine an oxidation reaction (occurring on the peroxidase-modified segment), a reduction reaction (occurring on the cytochrome c-modified segment), and an electron transfer in between their two segments (just as shown in Figure 3 for glucose oxidase and bilirubin oxidase). This cascade of events increased the diffusion coefficient of the hemeprotein-modified nanorods with 22% in a solution with 300 mU $mL^{-1}$ xanthine oxidase and 200 µM hypoxanthine as compared to the diffusion coefficient in water. The increase of the diffusion coefficient was sensitive to the substrate of xanthine oxidase used to generate the reactive oxygen species (hypoxanthine or xanthine) as well as to an inhibitor of xanthine oxidase (quercetin) (Figure 4). Moreover, the diffusion coefficient increased with 30% (over the value observed in water) when the nanorod was made electrically more conductive leaving thus no doubt that enzymatically-induced self-electrophoresis is involved [24]. Such peroxidase- and cytochrome c-modified nanorods represent an important step toward nanomotors which are able to rush to cells in oxidative stress and neutralize the reactive oxygen species causing problems.

Some of the above enzyme-based nanomotors are, in principle at least, able to pump liquid if they are immobilized into a fluid channel (because moving the liquid adjacent to their body remains the only option once they cannot move). However, turning an enzyme-based nanomotor into a pump was seldom carried out. Deoxyribonucleic acid (DNA) template - T4 DNA polymerase complexes show enhanced diffusive movement in the presence of their substrate, deoxy 2'-adenosine triphosphate, dATP (as detailed in the next section). When immobilized onto a spot of a fluidic channel, instead of moving they pump liquid at linear speed of up to 1.4 µm $s^{-1}$ in the presence of the mentioned substrate [26]. The ability of a spot of immobilized DNA polymerase complex to act as "pump" was explained by a density gradient that is established around the spot following the catalytic substrate conversion.

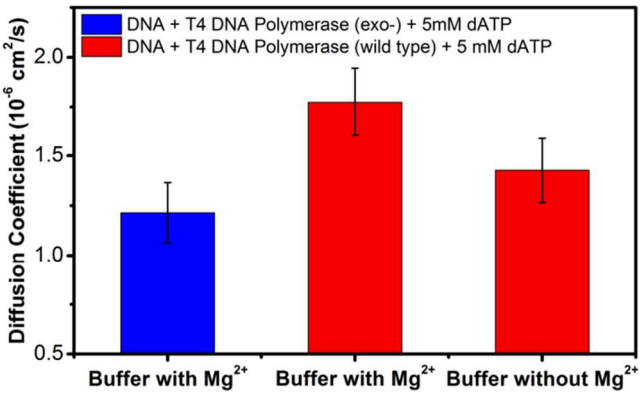


**Fig. 6** Diffusion coefficients of DNA polymerase complexes containing either the wild-type DNA polymerase or the exonuclease site mutant of DNA polymerase. *Important to note*: Wild-type DNA polymerase has catalytic activity while the mutant DNA polymerase has not. Therefore, the complex with the wild-type DNA polymerase shows an increase of 46% (17% without $Mg^{2+}$) over the diffusion coefficient of the complex with the mutant DNA polymerase. (Reprinted by permission from S. Sengupta, M. M. Spiering, K. K. Dey, W. Duan, D. Patra, P. J. Butler, R. D. Astumian, S. J. Benkovic, and A. Sen, ACS Nano, 2014, 8, 2410–2418. Copyright 2014 American Chemical Society)

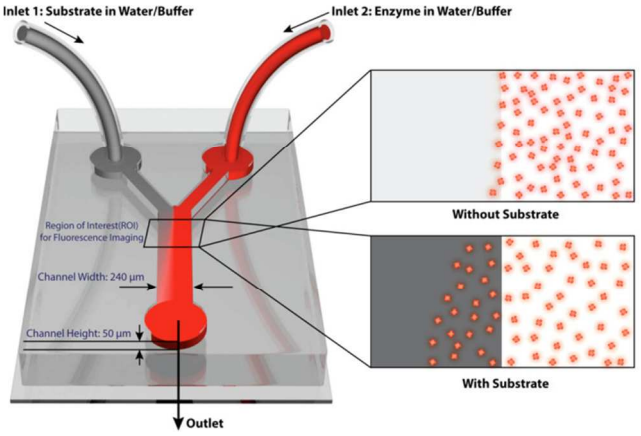


**Fig. 7** Schematic representation of the Y-shaped microfluidic channel used to observe the chemotaxis of enzyme molecules. *Important to note*: Because this microfluidic channel is characterized by a laminar flow, the enzyme solution introduced through inlet 2 will not significantly mix with solution introduced through inlet 1 unless this contains the enzyme substrate. (Reprinted by permission from S. Sengupta, K. K. Dey, H. S. Muddana, T. Tabouillot, M. E. Ibele, P. J. Butler, and Ayusman Sen, J. Am. Chem. Soc., 2013, 135, 1406–1414. Copyright 2013 American Chemical Society)

Similar enzymatic micropumps were very recently built with catalase, lipase, urease and glucose oxidase (Figure 5) [27]. Due to the very high activity of catalase, catalase-based micropumps provided one of the highest pumping speeds (4.51 µm $s^{-1}$), which was observed at hydrogen peroxide concentrations as high as 0.1 M. The ability of these pumps to turn ON when a given compound is present was also a little bit explored and exploited by building, an autonomous, glucose oxidase-powered pump that delivers insulin in response to glucose. In this pump, glucose oxidase and insulin were both immobilized into a hydrogel which was releasing insulin at higher speeds when glucose was available in higher concentrations.

Modification with enzymes is clearly a promising way both to achieve the autonomous motion of small objects and to pump liquid through microfluidic channels while maintaining increased compatibility with living systems. Interestingly, modification with enzymes also allows reproducing most of the mechanisms responsible for the self-propulsion of catalytic (i.e. non-enzymatic) nano- and micromotors.

## 3. Self-propulsion of freely-diffusing enzymes

Enzymatically induced motion was revealed by an unintentional top-down approach, that is, the self-propulsion of enzyme-modified nano- and microparticles was reported before the enhanced diffusive movement of enzyme-DNA complexes [26,27] and of enzyme molecules [29,30]. The enzymatically induced motion of nano- and microobjects was just reviewed in the previous section. This section will review the enhanced diffusive movement of freely-diffusing enzyme-DNA complexes and enzymes.

DNA-T7 RNA polymerase complexes were shown to enhance their diffusion coefficient in the presence of nucleoside triphosphates [28]. The enhanced diffusive movement of such complexes turns into directed motion (chemotaxis) when a gradient of nucleoside triphosphates appears. As shown in Figure 6, DNA template-T4 DNA polymerase complexes also increase their diffusion coefficient in the presence of dATP and $Mg^{2+}$ [26]. The ability of the DNA polymerase to act as "motor" was explained by the cycles of nonreciprocal conformational changes suffered by enzyme during catalytic cycles. Taking into account the large size of T4 DNA polymerase (898 amino acids, 103 kDa [31]), the conformational changes of T4 DNA polymerase during a catalytic cycle can indeed be quite significant. However, one can expect that the effectiveness of swimming by this mechanism is significantly reduced when the enzyme is small.

Researchers at The Pennsylvania State University were first to show that urease and catalase are also characterized by larger diffusion coefficients in the presence of their substrates than in the absence of their substrates [29,30]. Urease, the first ever enzyme crystallized [32], is another large enzyme made up of six subunits with ~ 90 kDa each [33]. It increases its diffusion coefficient in 100 mM urea with 28% as compared to the coefficient in the absence of urea [29]. Catalase increases its diffusion coefficient in 100 mM hydrogen peroxide with 45% as compared to the coefficient in the absence of hydrogen peroxide [30]. Interestingly, this increase is similar to the increase observed above for the DNA polymerase complex in 5 mM dATP. Moreover, just as the DNA-enzyme complexes, urease and catalase also "swim" toward regions with higher substrate concentrations. The microfluidic channel for observing this chemotaxis-like behavior of enzymes is schematically depicted in Figure 7. The exact mechanism causing enzymes to self-propel is still unclear. Changes in solution viscosity, temperature, and pH, and formation of bubbles due to the enzyme reaction were ruled out as possible causes for the self-propulsion of the enzymes. Both phoretic mechanism [29] and nonreciprocal conformational changes occurring during the catalytic cycle [30] were considered as the most plausible cause of the self-propulsion. Important to note, urease and catalase, just as

T4 DNA polymerase, are large enzymes. It can thus be expected that their conformational changes during catalytic cycles are indeed significant.

Self-propulsion is clearly a property of both enzyme-modified small objects and freely diffusing enzyme molecules exposed to an enzyme substrate concentration gradient. It is to be discovered if the mechanisms of self-propulsion of freely diffusing enzymes play a role also in the self-propulsion of enzyme-modified small objects.

## 4. Conclusions

Enzymatically induced motion (with enzymes which are not ATP-dependent motor proteins) was demonstrated at both single enzyme and enzyme-modified nano- and microobject level. DNA-enzyme complexes and enzymes were shown to enhance their diffusive movement in the presence of their substrates. Enzyme-modified nano- and microobjects were shown to present not only enhanced diffusive movement but also directed motion at speeds ranging from 0.119 μm $s^{-1}$ to 1 cm $s^{-1}$. These propulsion speeds were achieved by a variety of mechanisms including self-diffusiophoresis, recoil from bubbles, and self-electrophoresis. Using enzymes to develop an autonomous micropump able to move liquid at 4.51 μm $s^{-1}$ linear speed was also demonstrated. On the negative side we can notice that the enzyme-based nanomotors still require high fuel concentrations compared to the concentrations of these fuels in biological systems, move for a limited time, and / or their motion is restricted to the air-solution interface. We have definitively got closer to having tiny motors and pumps able to perform in living systems but we are not yet there.

How can we take enzymatically induced motion closer to applications (in biology)? A better understanding of the mechanism behind the enzymatically induced motion is definitively required. Engineering enzymes to show superior activity and better stability could also help. Enzyme-based nanomotors and micropumps developed up to now are based on few, relatively simple enzyme immobilization methods. These methods are easy to implement but they also tend to denaturate enzymes (negatively affecting their activity). Therefore, screening methods to immobilize different enzymes onto different locations of the same nano- or microobject, while maintaining enzyme activity, can also be part of the answer to the above question. Nanomotors moving through self-electrophoresis are in fact small short circuited batteries (fuel cells). Enzyme-based biofuel cells made already their way into the living body where they were able to perform for 110 days with no signs of rejection or inflammation [34]. Therefore, using some of (or getting inspiration from) the technical solutions developed for enzyme-based biofuel cells [35] could also help to develop better enzyme-based nanomotors.

What can we expect from enzymatically induced motion in the close future? The ultrasonic propulsion of rod-shaped Au nanomotors inside living cells was recently demonstrated [36]. Taking into account this achievement and those described above, enzyme-based nanomotors will certainly be deployed in the extra- and intracellular space of living cells. The motion of enzyme-based nanomotors is by default sensitive to biologically relevant molecules. Therefore, the easiest to imagine is that the motion of enzyme-modified nanorods will be used to monitor the concentration of such molecules inside and / or outside living cells with good spatiotemporal resolution.

## 5. Acknowledgements

The author thanks the Romanian Executive Unit for Higher Education, Research, Development and Innovation Funding for funding through grants PN-II-RU-TE-2011-3-0237, PN-II-CT-ERC-2012-1 (No. 9), and PN II-ID-PCCE-2011-2-0075.

## Notes and references

[a] *1B Intrarea Portocalelor, 060101 – Bucharest, Romania. Fax: + 40 21 3104361; Tel: + 40 21 3104354; E-mail: sgaspar@biodyn.ro*

1. J. Wang, ACS Nano, 2009, 3, 4–9.
2. T. Mirkovic, N. S. Zacharia, G. D. Scholes, and G. A. Ozin, Small, 2010, 6, 159–167.
3. W. Wang, W. Duan, S. Ahmed, T. E. Mallouk, and A. Sen, Nano Today, 2013, 8, 531–554.
4. L. K. E. A. Abdelmohsen, F. Peng, Y. Tu, and D. A. Wilson, J. Mater. Chem. B, 2013.
5. G. Loget and A. Kuhn, Nat. Commun., 2011, 2, Article number 535.
6. L. Baraban, R. Streubel, D. Makarov, L. Han, D. Karnaushenko, O. G. Schmidt, and G. Cuniberti, ACS Nano, 2013, 7, 1360–1367.
7. W. Gao, A. Pei, R. Dong, and J. Wang, J. Am. Chem. Soc., 2014, 136, 2276–2279.
8. D. A. Wilson, R. J. M. Nolte, and J. C. M. van Hest, Nat. Chem., 2012, 4, 268–274.
9. R. Liu and A. Sen, J. Am. Chem. Soc., 2011, 133, 20064–20067.
10. G. Zhao, M. Viehrig, and M. Pumera, Lab. Chip, 2013, 13, 1930–1936.
11. G. Zhao, H. Wang, B. Khezri, R. D. Webster, and M. Pumera, Lab. Chip, 2013, 13, 2937–2941.
12. H. Hess, G. D. Bachand, and V. Vogel, Chem. - Eur. J., 2004, 10, 2110–2116.
13. L. A. Cameron, M. J. Footer, A. van Oudenaarden, and J. A. Theriot, Proc. Natl. Acad. Sci., 1999, 96, 4908–4913.
14. P. Y. Chen and H. J. Keh, Journal of Colloid and Interface Science, 2005, 286, 774–791.
15. R. F. Ismagilov, A. Schwartz, N. Bowden, and G. M. Whitesides, Angew. Chem., 2002, 114, 674–676.
16. B. K. Vainshtein, W. R. Melik-Adamyan, V. V. Barynin, A. A. Vagin, and A. I. Grebenko, Nature, 1981, 293, 411–412.
17. J. Vicario, R. Eelkema, W. R. Browne, A. Meetsma, R. M. La Crois, and B. L. Feringa, Chem. Commun., 2005, 3936–3938.
18. S. Sanchez, A. A. Solovev, Y. Mei, and O. G. Schmidt, J. Am. Chem. Soc., 2010, 132, 13144–13145.
19. J. Simmchen, A. Baeza, D. Ruiz, M. J. Esplandiu, and M. Vallet-Regí, Small, 2012, 8, 2053–2059.
20. J. Orozco, V. García-Gradilla, M. D'Agostino, W. Gao, A. Cortés, and J. Wang, ACS Nano, 2013, 7, 818–824.
21. D. Pantarotto, W. R. Browne, and B. L. Feringa, Chem. Commun., 2008, 1533.
22. H. J. Hecht, H. M. Kalisz, J. Hendle, R. D. Schmid, and D. Schomburg, J. Mol. Biol., 1993, 229, 153–172.
23. N. Mano and A. Heller, J. Am. Chem. Soc., 2005, 127, 11574–11575.

24. I.-A. Pavel, A.-I. Bunea, S. David, and S. Gáspár, ChemCatChem, 2014, 6, 866–872.
25. A.-I. Bunea, I.-A. Pavel, S. David, and S. Gáspár, Chem. Commun., 2013, 49, 8803–8805.
26. S. Sengupta, M. M. Spiering, K. K. Dey, W. Duan, D. Patra, P. J. Butler, R. D. Astumian, S. J. Benkovic, and A. Sen, ACS Nano, 2014, 8, 2410–2418.
27. S. Sengupta, D. Patra, I. Ortiz-Rivera, A. Agrawal, S. Shklyaev, K. K. Dey, U. Córdova-Figueroa, T. E. Mallouk, and A. Sen, Nat. Chem., 2014, 6, 415–422.
28. H. Yu, K. Jo, K. L. Kounovsky, J. J. de Pablo, and D. C. Schwartz, J. Am. Chem. Soc., 2009, 131, 5722–5723.
29. H. S. Muddana, S. Sengupta, T. E. Mallouk, A. Sen, and P. J. Butler, J. Am. Chem. Soc., 2010, 132, 2110–2111.
30. S. Sengupta, K. K. Dey, H. S. Muddana, T. Tabouillot, M. E. Ibele, P. J. Butler, and Ayusman Sen, J. Am. Chem. Soc., 2013, 135, 1406–1414.
31. E. K. Spicer, J. Rush, C. Fung, L. J. Reha-Krantz, J. D. Karam, and W. H. Konigsberg, J. Biol. Chem., 1988, 263, 7478–7486.
32. J. B. Sumner, J. Biol. Chem., 1926, 69, 435–441.
33. K. Takishima, T. Suga, and G. Mamiya, Eur. J. Biochem., 1988, 175, 151–157.
34. A. Zebda, S. Cosnier, J.-P. Alcaraz, M. Holzinger, A. Le Goff, C. Gondran, F. Boucher, F. Giroud, K. Gorgy, H. Lamraoui, and P. Cinquin, Sci. Rep., 2013, 3.
35. M. T. Meredith and S. D. Minteer, Annu. Rev. Anal. Chem., 2012, 5, 157–179.
36. W. Wang, S. Li, L. Mair, S. Ahmed, T. J. Huang, and T. E. Mallouk, Angew. Chem., 2014, 126, 3265–3268.